Available online at www.sciencedirect.com
SCIENCE DIRECT®
Physics of the Earth and Planetary Interiors 149 (2005) 335–354
PHYSICS OF THE EARTH AND PLANETARY INTERIORS
www.elsevier.com/locate/pepi

Prediction of the *PVT* properties of water over wide range of temperatures and pressures from molecular dynamics simulation

Zhigang Zhang[a], Zhenhao Duan[a,b,*]

[a] *Chinese Academy of Sciences, Institute of Geology and Geophysics, Beijing 100029, China*
[b] *Department of Chemistry, 0340,University of California, San Diego, La Jolla, CA 92129, USA*

Received 24 August 2004; received in revised form 3 November 2004; accepted 8 November 2004

Abstract

In this study, we systematically performed a series of isothermal–isobaric molecular dynamics simulations over a wide range of temperatures and pressures to evaluate the pressure–volume–temperature (*PVT*) properties of water with four popular molecular potential, SPCE, TIP4P, TIP5P and EP. From the overview of the simulated data and their comparisons with experimental data, we find that SPCE shows overall better predictions than the other three models, slightly better than TIP4P, but far more accurate than EP and TIP5P. Compared with the most recent published high-pressure experimental data up to 5.0 GPa, the simulation results with SPCE show remarkable agreement with errors less than 1.0%. Considering this potential was proposed based on very few experimental data under room temperatures and pressures, the high accuracy of the simulation results indicate a great predictive power of molecular level study and verify our attempt of using molecular dynamics simulations to generate data as an important supplement to the database of experimental properties of geological fluids.

Based on our simulated data of SPCE and experimental data, a new equation of state (EOS) was proposed with better accuracy for the volumetric properties of liquid than previous models from 100.0 MPa and 273.15 K up to substantial ionization limit, which is about 20–30 GPa and 2000 K according to previous studies.

Keywords: Molecular dynamics; Water; High temperature and pressure; *PVT*; Equation of state; Geological fluids

1. Introduction

Water is known as the important member of many natural fluids and plays important roles in many processes, such as mineral deposits, volcanic eruptions, magmatic activities, metamorphism, hydrothermal venting, geothermal evolution, petroleum and natural gas formation and migration, and waste disposal. Consequently, knowledge of the thermodynamic properties of water is important for the interpretation of physical and chemical processes in the Earth's crust and mantle. Pressure–volume–temperature (*PVT*) properties can be used to construct an equation of state (EOS), which, in turn, can yield all kinds of thermodynamic properties including fugacity, enthalpy and volumetric

* Corresponding author.
E-mail address: duanzhenhao@yahoo.com (Z. Duan).

0031-9201/$ – see front matter © 2004 Elsevier B.V. All rights reserved.
doi:10.1016/j.pepi.2004.11.003

properties. Therefore, measuring the *PVT* properties of water has been an endeavor of many experimentalists.

Over the last century, a large number of experimental *PVT* data of water has been accumulated, but they are generally limited below 1273.15 K and 1.0 GPa (Sato et al., 1991). Newly developed techniques make it possible to extend experiments to 1873.15 K and about 5.0 GPa (Abramson and Brown, 2004; Brodholt and Wood, 1994; Frost and Wood, 1997; Larrieu and Ayers, 1997; Withers et al., 2000) but these experiments were still limited far below the Earth core temperature (>4000 K) and pressure (350 GPa). In the mean time, as the temperature and pressure increased, experiments become more and more difficult with noticeable uncertainties (Larrieu and Ayers, 1997). Shock wave measurements provide a routine to find the properties of compressed water under extreme temperatures and pressures (Kormer, 1968; Lyzenga et al., 1982; Mitchell and Nellis, 1982; Walsh and Rice, 1957). Nevertheless, this kind of measurements has an obvious disadvantage with imprecise temperature estimation.

Along with experimental work, various equations of state for water have been proposed. With elaborate calibrations of the parameters in these equations, some well established EOS can be used to accurately reproduce the experimental data (Duan et al., 1992a; Kerrick and Jacobs, 1981; Wagner and Prub, 2002). However, their extrapolation beyond experimental data range is limited.

Molecular dynamics/Monte Carlo (MD/MC) simulations have become increasingly powerful tools in the predicting of thermodynamic properties of geological fluids for the following reasons besides the increasingly more powerful computers: (1) MD/MC simulation depends little on experimental data and has far better predictability than such thermodynamic models as EOS. Molecular interaction potential (IP) is crucial in the simulation. The parameters of IP are generally evaluated from a few data points in a small *TP* space. Once the potential model is well established, it can be used to predict various thermodynamic, transport and liquid structure properties. However, it is the simulator's job to find out the validity of various potential models. That is also part of work in our study presented in this article. (2) Through MD/MC simulation, we can look into microscopic properties, which are generally difficult to observe experimentally. (3) There is no limitation on temperature, pressure and medium conditions, thus MD/MC is specially suitable for the study of the Earth and planets.

Because of the lack of *PVT* data for water at high temperatures and pressures and the advantages of MD/MC simulation in supplementing experimental data, in this study we try: (1) to evaluate the most frequently used potential models of water by extensive simulating the *PVT* properties over large *TP* space and to find the best potential model for the study of aqueous fluids; (2) to demonstrate the predictability of molecular dynamics simulation as "computer experiment" to produce thermodynamic data; (3) to establish an equation of state with higher accuracy than previous models up to the high pressure limit where water is substantially ionized.

As mentioned above, molecular potential is the key in the simulation. Over 40 potentials have been proposed for water but no one can be regarded as "perfect" to meet the insatiable appetites of different researchers (Guillot, 2002). Although polarization and many-body effect can be important in liquids, significant improvements has not been observed with state of art techniques (Finney, 2001). Therefore, pairwise additive potentials are still most frequently used in MD/MC simulations. Among the many pairwise additive potentials, SPCE (Berendsen et al., 1987) and TIP4P (Jorgensen et al., 1983) are the most widely used in various simulations as reviewed by (Kalinichev, 2001). However, there is apparent controversy about which is better than the other. Some studies indicate that TIP4P is better than SPCE, as indicated by the more realistic prediction of TIP4P in ice–ice–liquid phase diagrams than SPCE at low temperatures (Sanz et al., 2004). Other studies show clear advantages of SPCE over TIP4P. For examples, SPCE predicts more accurate liquid vapor phase equilibria and critical temperature and dielectric constants (Wasserman et al., 1994). It seems to us that SPCE has better predictions than TIP4P in the high *T–P* range and is more suitable for the study of salt–water mixtures. However, comprehensive evaluation of SPCE over a wide *T–P* range does not exist, while such work was done for the TIP4P model (Brodholt and Wood, 1993). In order to find the most appropriate potential for the study of *PVT* properties of water and aqueous mixtures, we make isothermal–isobaric molecular dynamics simulations using both TIP4P and SPCE potential. Since EP model (Errington and Panagiotopoulos, 1998) is considered

as most accurate in reproducing liquid–vapor phase equilibria and TIP5P (Mahoney and Jorgensen, 2000) is possibly superior to TIP4P, we also evaluate both EP and TIP5P with the isothermal–isobaric simulation technique over a large *TP* space.

In the next section, we briefly introduce the algorithm and equation of motion adopted in the isothermal–isobaric molecular dynamics simulations. Subsequently, simulation details with potential models and program setups are presented. Then, we make a careful discussion of the results and compare them with the experiments. Finally, some conclusions are drawn.

2. Simulation methodologies and algorithm

A number of algorithms for NPT ensemble have been proposed with thermostat and barostat variables added to the equations of motion (Andersen, 1980; Hoover, 1986; Martyna et al., 1994; Melchionna and Ciccotti, 1993; Nose, 1984). However, some of these algorithms were proved not reliable and may yield misleading or even pathological results according to the rigorous statistical mechanics in the non-Hamiltonian phase space (Tuckerman et al., 2001). For example, according to the analysis of Tuckerman et al. (2001) and our own experience, if the algorithm presented in Hoover (1986) was adopted, an erroneous volume distribution would be generated and the averaged pressure would be systematically larger than the desired value. As a result, in this study we adopted an improved algorithm suggested by Martyna et al. (1994), which has the following form:

$$\ddot{r}_i = \frac{F_i}{m_i} + \dot{\eta}^2 r_i + \ddot{\eta} r_i - \left(\xi + \frac{3\dot{\eta}}{f}\right)(\dot{r}_i - \dot{\eta} r_i) \tag{1a}$$

$$\ddot{\eta} = \frac{(P_{\text{inst}} - P_{\text{desire}})\exp(3\eta)}{t_p^2 k_B T_{\text{desire}}} + \frac{\sum_{i=1}^{N} m_i(\dot{r}_i - \dot{\eta} r_i)^2}{f t_p^2 k_B T_{\text{desire}}} - \xi\dot{\eta} \tag{1b}$$

$$\dot{\xi} = \frac{\sum_{i=1}^{N} m_i(\dot{r}_i - \dot{\eta} r_i)^2 + 3\dot{\eta}^2 t_p^2 k_B T_{\text{desire}} - (f+1) k_B T_{\text{desire}}}{Q} \tag{1c}$$

$$\eta = \ln V^{1/3} \tag{1d}$$

where r_i, F_i and m_i are the position, force and mass of the ith particle, respectively; ξ and η the thermostat and barostat variables, respectively, with two corresponding parameters of Q and t_p to adjust the fluctuation of temperature and pressure; V the volume; f the degree of freedom of the simulated system with N particles; k_B the Boltzmann constant; P_{desire} and T_{desire} the desired/external pressure and temperature, respectively; P_{inst} is the instantaneous pressure, which is calculated from atomic virial $W = \frac{1}{3}\sum_i F_i \cdot r_i$ (Ciccotti et al., 2001):

$$P_{\text{inst}} = \frac{1}{3V}\sum_{i=1}^{N} m_i(\dot{r}_i - \dot{\eta} r_i)^2 + \frac{W}{V} \tag{2}$$

Eqs. (1a)–(1d) and (2) have an apparently different form from that presented in Martyna et al. (1994) for the convenience of our programming but can easily found to be entirely equivalent. The velocity of particle v_i is related with the time derivative of position r_i by:

$$v_i = \dot{r}_i - \dot{\eta} r_i \tag{3}$$

We did not write this variable explicitly in Eqs. (1a)–(1d) and (2) for the sake of clarity and more importantly, we found that with the time derivative of position rather than the velocity it is more straightforward to integrate the equations of motion (Eqs. (1a)–(1d)) with velocity Verlet algorithm (Swope et al., 1982), which is described in detail in Appendix A.

3. Simulation details

As stated in the introduction, over 40 potential models have been proposed. Evaluations and comparisons between these potential models can be easily found in a list of excellent reviews (e.g. Finney, 2001; Guillot, 2002; Head-Gordon and Hura, 2002; Kalinichev, 2001; Wallqvist and Mountain, 1999 and references therein). For the reasons we mentioned in the introduction, we try to identify the best potential for the study of water in the high *T*–*P* region from SPCE, EP, TIP4P and TIP5P.

The geometries and parameters for SPCE, EP, TIP4P and TIP5P models can be found in their original publications. We give a brief description here: SPCE has triangle geometry with OH bond length constrained to be 1.0 Å and the angle H–O–H fixed as 109.47°; EP

model has the same HOH angle but slightly enhances the bond length of OH to be 1.0668 Å; the HOH geometries of TIP4P and TIP5P differ from SPCE with OH bond length constrained to be 0.9572 Å and the H–O–H angle fixed as 104.52°, respectively. In both models of TIP4P and TIP5P, the oxygen atom is neutral and extra force centers (denoted as M) are designed to carry negative charges. For TIP4P, this center is located at the bisector of H–O–H angle and 0.15 Å away from the oxygen atom; while for TIP5P the extra force centers are positioned at the lone-pair sites of oxygen atom with OM bond length to be 0.70 Å and the angle M–O–M fixed as 109.47°. The potential functions for these models can be formulated as a summation of short-range interaction between oxygen atoms and Coulombic interaction between charges:

$$u(1,2) = u_{\text{short}}(r_{\text{OO}}) + u_{\text{Coul}}(1,2) = u_{\text{short}}(r_{\text{OO}}) + \sum_{i\in\{1\}}\sum_{j\in\{2\}}\frac{q_i q_j}{r_{ij}} \quad (4)$$

where r_{OO} is the distance of two oxygen atoms and r_{ij} is the separation between two interaction charges with partial charges of q_i and q_j. For SPCE, TIP4P and TIP5P, short-range interactions are calculated with Lennard–Jones function:

$$u_{\text{short}}^{\text{LJ}}(r_{\text{OO}}) = 4\varepsilon_{\text{O}}\left[\left(\frac{\sigma_{\text{O}}}{r_{\text{OO}}}\right)^{12} - \left(\frac{\sigma_{\text{O}}}{r_{\text{OO}}}\right)^{6}\right] \quad (5)$$

while EP adopts a more complex function of Buckingham exponential-6 potential:

$$u_{\text{short}}^{\text{exp-6}}(r_{\text{OO}}) = \frac{\varepsilon_{\text{O}}}{1-6/\alpha}\left[\frac{6}{\alpha}\exp\left(\alpha\left[1-\frac{r_{\text{OO}}}{r_m}\right]\right) - \left(\frac{r_m}{r_{\text{OO}}}\right)^{6}\right] \quad (6)$$

where ε_{O} is the energy parameters for short-range interactions, σ_{O} is the size parameter for Lennard–Jones potential and r_m and α are parameters for exponential-6 potential. For exponential-6 potential, an equivalent value of σ_{O} can be computed by solving $u_{\text{short}}^{\text{exp-6}}(r_{\text{OO}}) = 0$. All of these parameters and geometries are summarized in Table 1.

In all of our molecular dynamics simulations, 256 water molecules were placed in the simulation box. The conventional periodic boundary conditions and minimum image conventions (Allen and Tildesley, 1989) were used in the simulations to calculate inter-atom distances. Long-range electrostatic forces and energies were calculated with the Ewald summation. Long-range corrections to the Lennard–Jones interactions were made with the formulations presented in Zhang and Duan (2002). Velocity Verlet algorithm (Swope et al., 1982) was adopted to propagate the statistical trajectory, which is described in detail in the Appendix A. The geometries of the HOH atoms in water were constrained with the RATTLE method (Andersen, 1983). The positions of the extra force centers in TIP4P and TIP5P models vary with those of primary HOH atoms with the method suggested in Ciccotti et al. (1982). Notice that the forces acting on the extra force centers and the corresponding atomic virials should be carefully transformed to the primary HOH atoms for consistence. Parameters of Q and t_p in Eqs. (1a)–(1d) were adjusted to control the fluctuation of temperature and pressure according to the suggestion of Martyna et al. (1994), with a typical value of 5.0 kJ ps^2/mol for Q and 5.0 ps for t_p. The time step of all the simulations was set as 1.0 fs. Simulations were initiated from the configurations "melted" from the face-centered cubic lattice structure or the previous equilibrated configurations at similar densities. The instantaneous volumes were recorded and counted into the statistical average for about 50 ps after a 10–20 ps pre-equilibrium simulation. At lower temperatures and pressures, longer simulations (to 80 ps) were performed to ensure the convergence of the simulation and sufficient statistical reliability.

Table 1
Parameters and geometries for different potential models

	SPCE	TIP4P	TIP5P	EP
$\varepsilon_{\text{O}}/k_{\text{B}}$ (K)	78.073	78.021	80.52	159.78
σ_{O} (Å)	3.166	3.154	3.12	3.195
α	–	–	–	12.0
q_{O} (e)	−0.8476	0	0	0.7374
q_{H} (e)	0.4238	0.52	0.241	0.3687
q_{M} (e)	–	−1.04	−0.241	–
O—H (Å)	1.0	0.9572	0.9572	1.0668
O—M (Å)	–	0.15	0.70	–
H—O—H (°)	109.47	104.52	104.52	109.47
M—O—M	–	–	109.47°	–

4. Results and discussion

4.1. Reliability

Before presenting the simulation results, we briefly evaluate the reliability of our simulation results, which involves three aspects: uncertainty estimations, check of possible finite size effect and consistence analysis between our simulation results and the prior workers.

As described in the previous section, the simulation algorithm adopted in this study mimics the real experimental conditions by a kind of bath coupling with a thermostat and barostat. Consequently, the temperatures and pressures will inevitably waggle around the desired values with fluctuations. With careful adjustment of the thermostat and barostat parameters, the uncertainties involved in these fluctuations can be controlled in an acceptable tolerance. We estimated these uncertainties with the statistical standard deviations by dividing a whole run into 10 blocks discarding the pre-equilibrium stages (Allen and Tildesley, 1989). When temperatures and pressures increased, the fluctuations would generally be enlarged. Nevertheless, the uncertainties in the temperatures and pressures can be safely claimed to be less than 2.0 K and 10.0 MPa.

In order to show the possible finite size effect and adequacy of our simulation length, a listed of simulations with different system sizes and simulation times were carried out and the simulated volumes were tabulated in Table 2. From this table, we find that almost all of the simulated volumes are consistent with each other within their uncertainties. Simulations with larger system size and longer simulation time generally reduce the uncertainties but this effect seems to be marginal.

Table 2
Illustrative simulations at 5000.0 MPa and 673.15 and 623.15 K to show the finite size effect and adequacy of simulation time

System size	Simulation time (ps)	673.15 K	623.15 K
108	50	12.49(.03)[a]	12.35(.02)
256	50	12.47(.01)	12.35(.02)
512	50	12.48(.01)	12.35(.01)
108	80	12.48(.03)	12.34(.02)
256	80	12.47(.01)	12.35(.01)
512	80	12.47(.01)	12.35(.01)
108	100	12.48(.02)	12.34(.02)
256	100	12.47(.01)	12.35(.01)
512	100	12.47(.01)	12.35(.01)
108	200	12.47(.01)	12.34(.01)
256	200	12.48(.01)	12.35(.01)
512	200	12.48(.01)	12.35(.01)

Note: volumes in cm^3/mol.
[a] The numbers in the parentheses are the uncertainties. For example, 12.49(.03) means 12.49 ± 0.03.

A large number of publications exist with the simulation results utilizing SPCE, TIP4P and TIP5P. However, the reported data are not always consistent with each other for the sake of different simulation details. For example, for some historical reasons, the early workers roughly dealt with the long-range forces by simply cutting-off without any corrections and this kind of treatment turned out to have possibilities of generating erroneous results. Table 3 lists our simulation

Table 3
Simulation results at 298.15 K and 0.101325 MPa (1.0 atm) in this study and a comparison with those of prior workers

	SPCE		TIP4P		TIP5P	
	This study	Ref.	This study	Ref.	This study	Ref.
ρ (g/cm^3)	0.997 ± 0.008	0.998[a] 0.9986[d]	0.990 ± 0.004	0.999[b] 0.9935[d]	0.983 ± 0.004	0.999[c] 0.9834[e] 0.9826[d]
$-E$ (kcal/mol)	11.17 ± 0.03	11.14[a,f] 11.1310[d]	9.89 ± 0.03	10.07[b] 9.8559[d]	9.61 ± 0.03	9.87[c] 9.665[e] 9.5918[d]

Note: density (ρ) and configuration energy (E) at 300 K.
[a] Berendsen et al. (1987).
[b] Jorgensen et al. (1983).
[c] Mahoney and Jorgensen (2000).
[d] Paschek (2004).
[e] Lisal et al. (2002).
[f] Without self-energy correction.

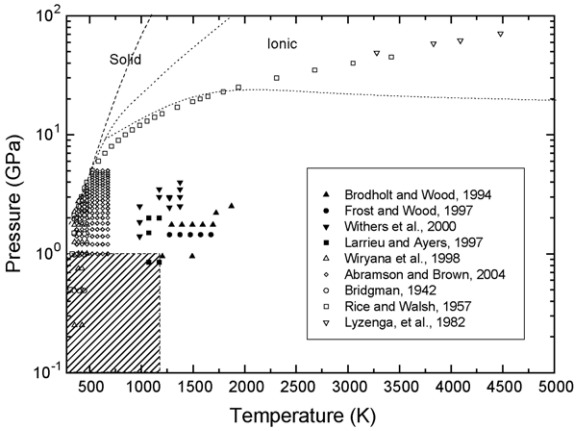

Fig. 1. Experimental *PVT* data available projected in the *TP* space. The left bottom area enclosed by dashed line denotes the commonly measured region with temperature less than 1273.15 K and pressure less than 1.0 GPa. Two dotted lines determined from first principle simulations are set to separate different phase status of water (Cavazzoni et al., 1999). Experimental melting line was drawn with dashed line (Franck et al., 2004).

results at 298.15 K and 0.101325 MPa (1.0 atm) and gives a comparison with those of some prior workers. We notice that our simulation results are in very good agreement with most of recent references but slightly deviate from those of Jorgensen et al. (1983) and Mahoney and Jorgensen (2000). This kind of deviation can attribute to our Ewald treatment of long-range forces (Lisal et al., 2002).

4.2. A brief review of experimental data

Fig. 1 shows the experimental data available distributed in the *TP* space. In the bottom left corner of the figure (indicated by shadowed region, $T < 1273.15$ K and $P < 1.0$ GPa), abundant *PVT* data have been accumulated for the widely industrial interests in this region (Sato et al., 1991). The International Association for the Properties of Water and Steam (IAPWS) has proposed a well established and widely accepted equation of state for water properties in this region (so-called IAPWS95) and they claimed this equation could reproduce *PVT* properties in very good agreement with the experiments (Wagner and Prub, 2002). As a result, in this region we directly regard the data calculated from IAPWS95 as the experimental data in the following descriptions.

For pressures above 1.0 GPa, experimental data are approximately distributed in two regions. The first group ranges from 298.15 to 673.15 K and was available early in 1942 with Dr. Bridgman as the original contributor (Bridgman, 1942). Compressions of liquid water under temperatures to 448.15 K and pressures up to 3.58 GPa could be found in his paper. Another contributor in this area was the group of Brown (Abramson and Brown, 2004; Wiryana et al., 1998), who measured the velocities of sound in water and derived the *PVT* properties up to 673.15 K and 5.0 GPa. The second group ranges from 983.19 to 1873.15 K with newly developed techniques (Brodholt and Wood, 1994; Frost and Wood, 1997; Larrieu and Ayers, 1997; Withers et al., 2000). Some noticeable uncertainties exist in these data and this urges us to carefully analyze their consistence.

As far as we know, there is no static measurement of the *PVT* properties of water under higher temperatures and pressures than those described above. In the extreme *T–P* range, dynamical shock wave experiments may serve as the only routine to uncover the properties of water despite that there are doubts on whether these measurements describe equilibrium states at all (Wagner and Prub, 2002). Early in the year of 1957, Walsh and Rice (1957) published the shock wave measurement at relatively lower temperatures and pressures (to 41.9 GPa). Lyzenga et al. (1982) and Mitchell and Nellis (1982) extended the shock wave data to 83.16 GPa. One difficulty involved in the comparison between our simulations and shock wave data is the uncertainties of temperature estimations. Several papers devoted to calculate the temperatures with theoretical theories but later turned out to be not reliable or model dependent (Ree, 1982; Rice and Walsh, 1957). Independent measurements of temperatures with optical studies include Kormer (1968) and later Lyzenga et al. (1982).

At extreme high temperatures and pressures, the water molecules tend to significantly dissociate (ionize) into hydrogen (or hydronium) and hydroxide (Hamann, 1981). It's hard to determine when this kind of reaction dominates in the bulk water from experiments. With the aid of ab initio simulations, Cavazzoni et al. (1999) suggested a possible region of ionic and superionic water, the boundary of which is marked in Fig. 1 as dotted lines. As revealed in our following descriptions, this would be important to interpret some deviations

of simulated data from experiments. For comparison, experimental melting line is also drawn in Fig. 1 as a dashed line (Franck et al., 2004).

4.3. Simulation results

A serial of simulations (over 200 data points for each potential model ranging from 273.15 to 4273.15 K and from 0.1 MPa to 50 GPa) has been performed to systematically evaluate the *PVT* properties of SPCE, TIP4P, TIP5P and EP models. For convenience, we gave our analyses of the simulation results in three parts.

4.3.1. In the region of $T < 1273.15$ K, $P < 1.0$ GPa

In order to give an overview of the evaluations in this region, we present in Fig. 4 the plots of the relative errors distributed in this *T–P* range for the four models.

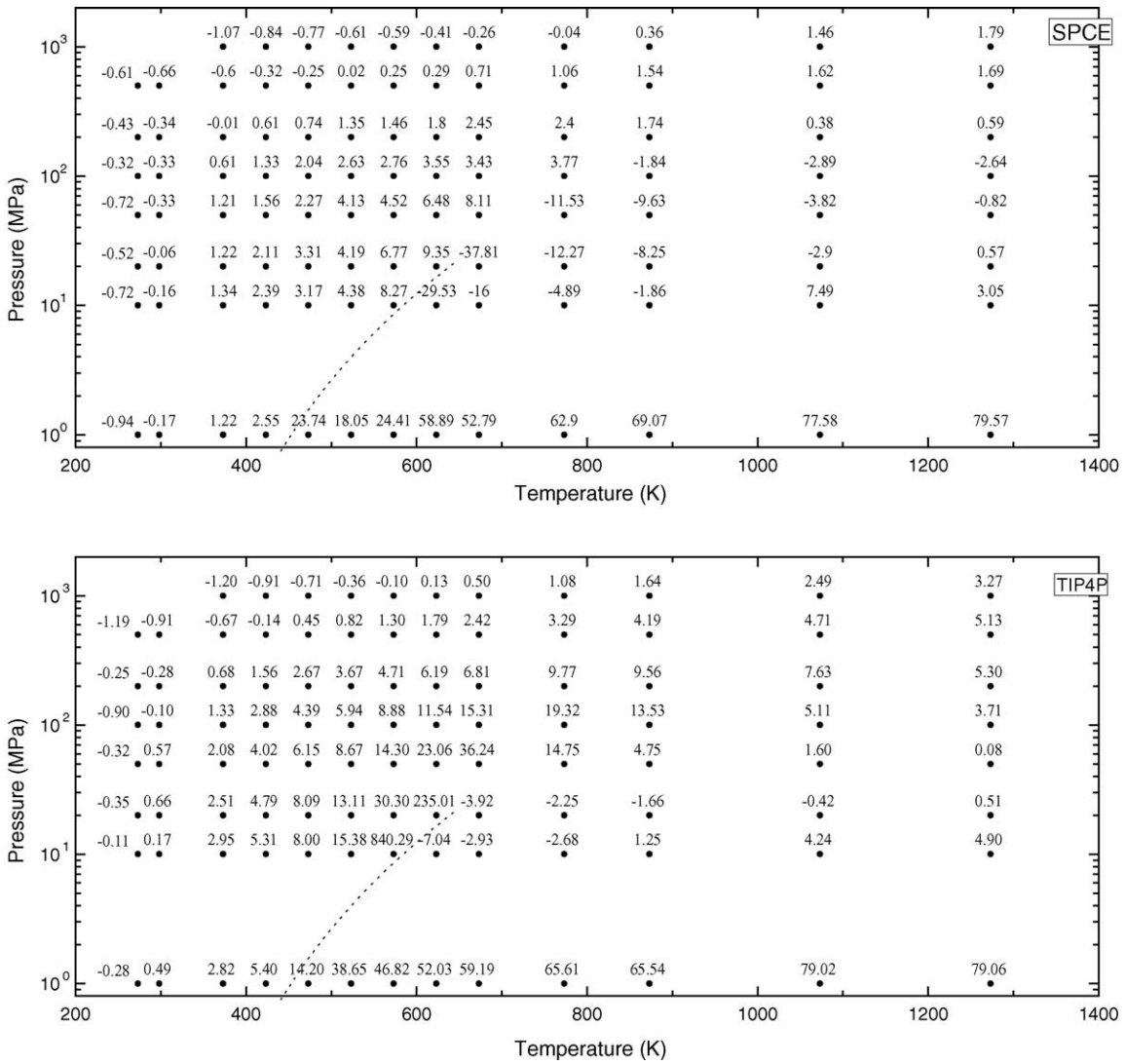

Fig. 2. Relative errors of the three models distributed in the *T–P* range of 273.15–1273.15 K and 0–1.0 GPa. Logarithmic axes for pressures were adopted for clarity. The relative errors were labeled on the top of each dot denoting the corresponding simulation conditions. Dotted curve indicates the experimental liquid–vapor coexistence line of water.

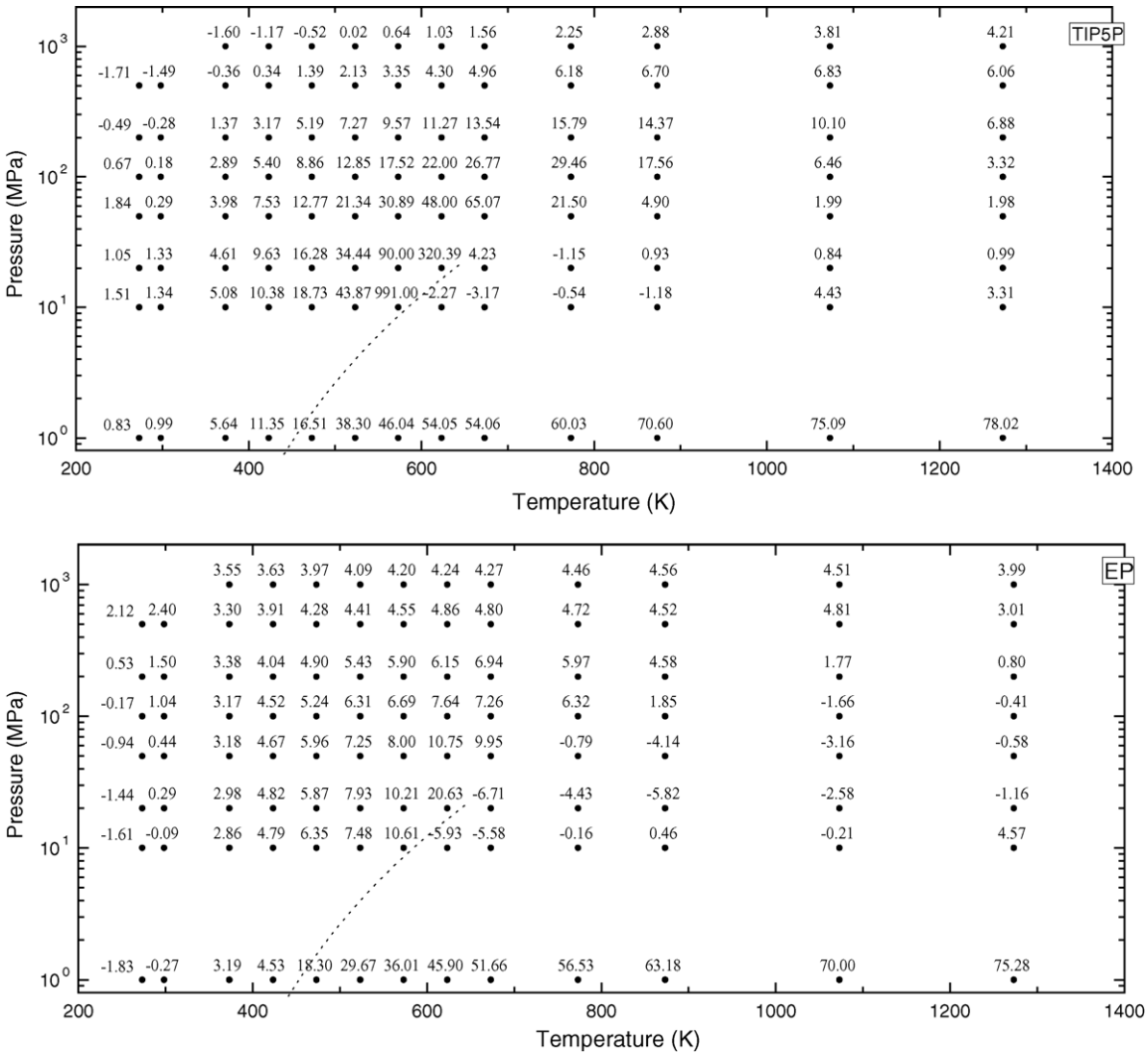

Fig. 2. (*Continued*).

Relative error was defined as:

$$\mathrm{Err}\% = \frac{V_{\mathrm{sim}} - V_{\mathrm{exp}}}{V_{\mathrm{exp}}} \times 100\% \quad (7)$$

where V_{sim} and V_{exp} are the simulated volume and the corresponding experimental volume, respectively.

From Fig. 2, SPCE shows overall better reproduction of the experimental *PVT* data of liquid and compressed water. TIP5P, which was claimed to be a better choice in the existing pairwise additive models (Mahoney and Jorgensen, 2000), was unfortunately proved to be even inferior to its predecessor, TIP4P, in this region. EP, which was original proposed to reproduce accurate phase equilibrium, shows better behavior in the gaseous region but generally overestimates the volumes of liquid water.

We notice some general features implied in the four plots of Fig. 2. First of all, in the vicinity of liquid–vapor coexistence curve (indicated as dotted curve) some prominent errors can be found. This is understandable for two reasons: firstly, in this region and especially when approaching the critical point, the simulation itself carries larger uncertainties; secondly,

the coexistence lines of the models may differ from those of real water.

The second common feature in the four profiles of Fig. 2 is the quite large deviations the simulated vapor density from experimental data at low pressures (below 10 MPa), which indicates a complete failure of these models for vapor. The significant overestimation may attribute to the enhanced dipole moment used in these models and also the imprecise modeling of the attractive interactions. By contrast, some simple spherical models are found to show their advantages of remarkable accuracies (Belonoshko and Saxena, 1991; Duan et al., 1996).

4.3.2. In the higher pressure region

Simulated *PVT* properties under higher temperatures and pressures are tabulated in Table 4. Also presented are the uncertainties of simulated volumes in

Table 4
Simulated *PVT* properties for different models

T (K)	*P* (MPa)	SPCE	TIP4P	TIP5P	EP	Exp.	Ref.
1203.15	950	22.38(.14)[a]	22.74(.17)	22.91(.16)	22.90(.15)	22.56(.36)	Brodholt and Wood (1994)
1293.15	1750	18.89(.07)	19.02(.07)	19.12(.07)	19.36(.05)	19.15(.19)	Brodholt and Wood (1994)
1393.15	1750	19.45(.06)	19.61(.06)	19.71(.13)	19.93(.07)	19.54(.33)	Brodholt and Wood (1994)
1491.15	950	25.36(.20)	25.78(.18)	26.10(.23)	25.82(.10)	25.86(.61)	Brodholt and Wood (1994)
1493.15	1750	20.13(.10)	20.23(.11)	20.29(.12)	20.44(.08)	20.49(.24)	Brodholt and Wood (1994)
1593.15	1750	20.68(.09)	20.82(.10)	20.86(.06)	21.01(.07)	21.47(.29)	Brodholt and Wood (1994)
1693.15	1750	21.29(.13)	21.38(.17)	21.45(.09)	21.55(.10)	21.79(.30)	Brodholt and Wood (1994)
1723.15	2200	19.68(.09)	19.78(.07)	19.74(.10)	19.94(.05)	20.15(.37)	Brodholt and Wood (1994)
1873.15	2500	19.45(.10)	19.49(.09)	19.53(.04)	19.61(.09)	19.61(.31)	Brodholt and Wood (1994)
1273.15	1450	19.91(.05)	20.1(.05)	20.19(.07)	20.43(.08)	20.03(.26)	Frost and Wood (1997)
1373.15	1450	20.62(.05)	20.80(.05)	20.89(.05)	21.07(.08)	20.83(.25)	Frost and Wood (1997)
1473.15	1450	21.31(.07)	21.54(.06)	21.63(.04)	21.73(.09)	21.6(.28)	Frost and Wood (1997)
1573.15	1450	22.06(.05)	22.26(.07)	22.35(.08)	22.39(.13)	22.3(.33)	Frost and Wood (1997)
1673.15	1450	22.79(.07)	23.01(.09)	23.01(.08)	23.09(.10)	23.15(.32)	Frost and Wood (1997)
983.15	1850	16.84(.06)	16.88(.04)	16.92(.07)	17.38(.04)	16.98	Withers et al. (2000)
983.15	1400	18.06(.07)	18.17(.05)	18.32(.08)	18.66(.03)	18.18	Withers et al. (2000)
983.15	2500	15.61(.02)	15.62(.04)	15.64(.03)	16.11(.02)	15.79	Withers et al. (2000)
1173.15	3000	15.65(.04)	15.65(.03)	15.65(.04)	16.05(.03)	15.79	Withers et al. (2000)
1173.15	3500	15.03(.03)	15.02(.05)	15.02(.04)	15.40(.01)	15.38	Withers et al. (2000)
1273.15	3000	16.04(.03)	16.05(.04)	16.02(.03)	16.40(.03)	16.22	Withers et al. (2000)
1273.15	2950	16.10(.05)	16.10(.07)	16.10(.04)	16.48(.03)	16.27(.18)	Withers et al. (2000)
1273.15	2450	16.97(.07)	17.06(.04)	17.02(.06)	17.38(.05)	16.69(.13)	Withers et al. (2000)
1373.15	3000	16.40(.04)	16.39(.05)	16.36(.03)	16.73(.02)	16.51	Withers et al. (2000)
1373.15	4000	15.10(.04)	15.09(.03)	15.08(.04)	15.40(.03)	15.25	Withers et al. (2000)
1373.15	2500	17.29(.08)	17.34(.06)	17.33(.05)	17.66(.04)	17.31	Withers et al. (2000)
1373.15	3500	15.69(.03)	15.67(.05)	15.68(.03)	16.01(.02)	15.65	Withers et al. (2000)
1073.15	850	21.84(.14)	22.12(.15)	22.35(.15)	22.43(.11)	21.63(1.21)	Larrieu and Ayers (1997)
1073.15	2000	16.94(.05)	17.06(.06)	17.07(.03)	17.48(.03)	17.19(.31)	Larrieu and Ayers (1997)
1073.15	1500	18.30(.08)	18.51(.08)	18.56(.08)	18.89(.04)	18.52(.09)	Larrieu and Ayers (1997)
1173.15	2000	17.49(.07)	17.55(.05)	17.61(.06)	17.97(.05)	17.65(.29)	Larrieu and Ayers (1997)
1173.15	850	22.89(.21)	23.29(.15)	23.54(.18)	23.44(.12)	23.54(.25)	Larrieu and Ayers (1997)
623.15	2000	14.66(.02)	14.65(.02)	14.65(.02)	15.31(.01)	14.74	Rice and Walsh (1957); Abramson and Brown (2004)
623.15	5000	12.35(.01)	12.29(.01)	12.20(.01)	12.77(.01)	12.35	Rice and Walsh (1957); Abramson and Brown (2004)
673.15	2000	14.90(.02)	14.91(.02)	14.93(.03)	15.54(.02)	14.97	Rice and Walsh (1957); Abramson and Brown (2004)
673.15	5000	12.48(.01)	12.43(.01)	12.34(.01)	12.89(.02)	12.47	Rice and Walsh (1957); Abramson and Brown (2004)

Note: volumes in cm^3/mol.

[a] The numbers in the parentheses are the uncertainties. For example, 22.38(.14) means 22.38 ± 0.14.

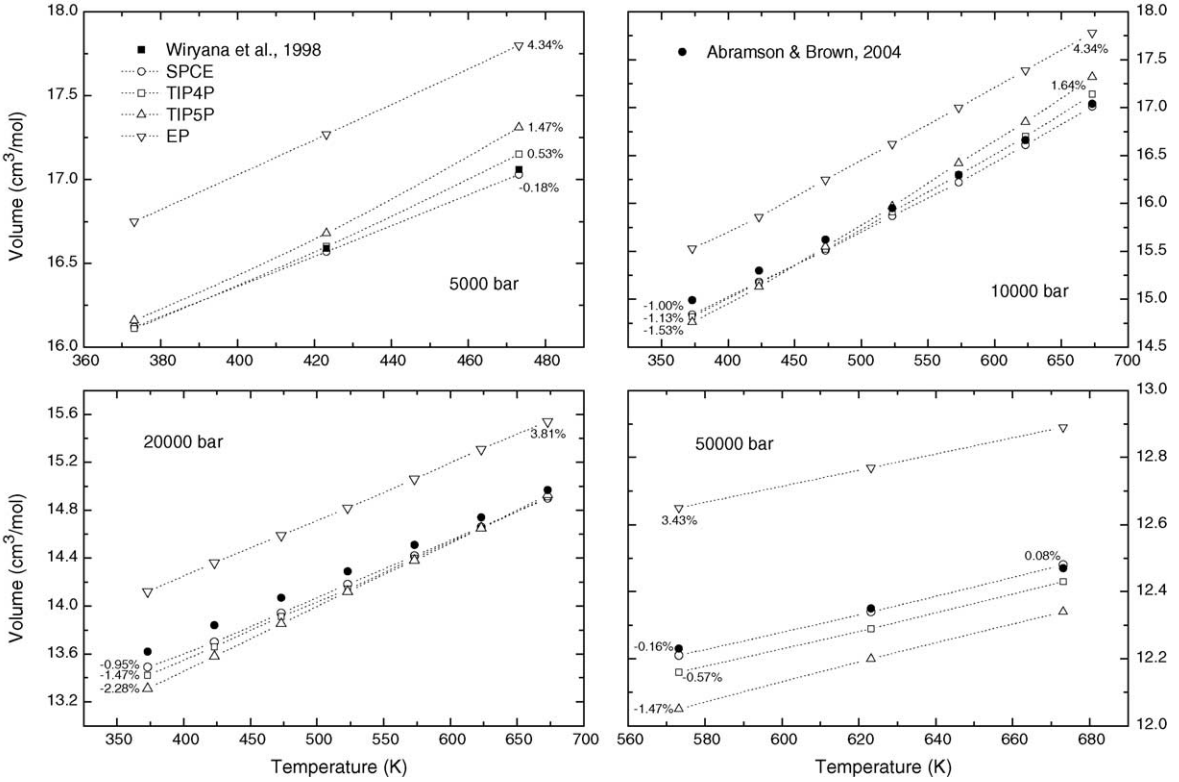

Fig. 3. Simulated volumes at high pressures from 0.5 to 5.0 GPa and comparisons with the experiments (Abramson and Brown, 2004; Wiryana et al., 1998). The numbers labeled in the vicinities of the simulated data points were the errors relative to corresponding experimental data.

the parentheses, which were estimated with the same method of temperature and pressure uncertainties estimation mentioned above, and the experimental uncertainties. In this region, the water molecules rotate faster and the boring hydrogen bonding and many body effects are gradually smoothed. The interactions become simpler and consequently the simulated results of four models are found to be comparative and are generally within the experimental uncertainties.

Fig. 3 shows comparisons between the simulated volumes and a set of most recent experimental high-pressure data from 0.5 to 5.0 GPa (Bridgman, 1942; Wiryana et al., 1998). EP model again shows significant overestimation of volume in this region while SPCE gives remarkable predictions with relative errors within 1.0%. TIP4P and TIP5P also generate data with good accuracies but deviate more from experiments than SPCE.

Fig. 4 reveals a general trend by projecting all the simulated data into a plot showing the relative errors varying with the corresponding pressures and volumes. From Fig. 4a, an obvious trend of being more accurate towards higher pressures could be found for SPCE, TIP4P and TIP5P. This is an encouraging feature for the molecular level study of geological fluids if we keep in mind that these models were originally calibrated from data at normal pressures. This feature is further verified in Fig. 4b, which shows better accuracy at compressed state for SPCE, TIP4P and TIP5P. On the other hand, EP generally shows overestimations at high pressures and condensed states. From this figure and Fig. 2, we can conclude: (1) molecular dynamics simulations can generate quite accurate data if we carefully select an appropriate interaction potential and this kind of predictability can be extended far beyond the thermodynamic conditions under which the potential model was calibrated; (2) the SPCE model is very suitable for the prediction properties under geological thermodynamic conditions by noticing its generally increased accuracies towards higher pressures and compressed

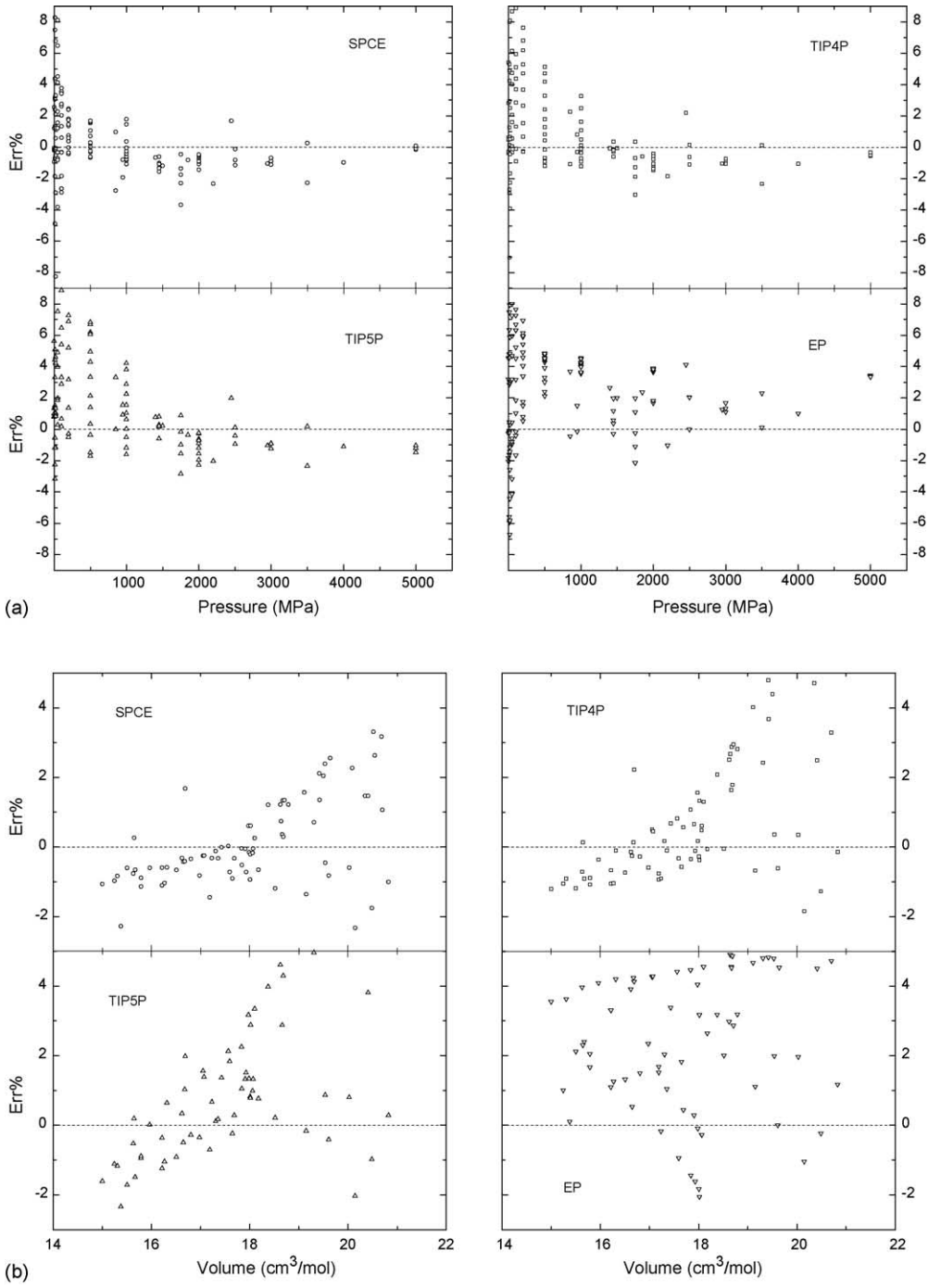

Fig. 4. Projections of all the simulated data into a plot with their relative errors for different pressures (a) and volumes (b).

densities, although TIP4P can also serve as such a purpose with slightly less accuracy; (3) simple modifications on the potential models of SPCE and TIP4P seem to be discouraging from the overall inaccuracy of EP, which shows truly improved phase behaviors but actually sacrifices the accuracy of volumetric properties.

4.3.3. Comparison with the shock wave measurements

How far beyond the data of 5.0 GPa and 1873 K can we explore the *PVT* profiles of water with these empirical pairwise additive potentials? It is hard to give an accurate answer for the scarcity of experimental data. Nevertheless, we may seek some implications from the shock wave measurements.

A detailed description of the shock wave measurements can be found in a list of publications dealing with high-pressure experiments (e.g. McQueen et al., 1970). This kind of measurements involves a sudden traverse of the shock front to a mass element and results in an almost discontinuous change of the thermodynamic states. Meanwhile, the thermodynamic properties should obey a number of conservation laws, which is called Rankine–Hugoniot relations. One of these relations is useful for our evaluation and has the following form (McQueen et al., 1970):

$$E_1 - E_0 = \frac{1}{2}(P_1 + P_0)(V_0 - V_1) \tag{8}$$

where P_0, V_0, E_0 and P_1, V_1, E_1 denote pressure, specific volume and specific internal energy ahead of and behind the shock front, respectively.

An obvious difficulty in our comparison with shock wave measurements is the imprecise estimation of the shock temperatures. As a result, we performed "computer shock wave experiments" and found several data points with thermodynamic properties obeying Eq. (8). In order to accomplish this target, we first selected the initial state with $P_0 = 0.101325$ MPa and $T_0 = 295.8$ K, which corresponds to that of the shock wave measurements (Ree, 1982). In order to get a target pressure, we started our exploration of the corresponding volume with a temperature theoretically calculated by Rice and Walsh (1957) or experimentally measured by Lyzenga et al. (1982). By slowing calibrations of the temperatures and with the help of some reliable interpolations, we found the final points on the Hugoniot curve.

The final simulated Hugoniot *P–V* and *T–P* curves are shown in Fig. 5. From this figure, we find that the Hugoniot curves for the three models of SPCE, TIP4P and TIP5P show similar behaviors. At lower temperature and pressure, our simulated data point can be well merged into the shock wave data (Lyzenga et al., 1982; Mitchell and Nellis, 1982; Walsh and Rice, 1957). But when temperature increased to about 2000 K and pressure up to 20.0 GPa, the simulated Hugoniot curves gradually deviate from the experimental curves. Similar deviations were observed by Guillot and Guissani (2001) in their simulations. One possible interpretation is related to the dominant water dissociation effect in this region, which is confirmed by some experimental implications (Hamann, 1981) and the most recent first principle simulations (Cavazzoni et al., 1999; Schwegler et al., 2001).

4.4. Equation of state

Equations of state formulate the relationship between the pressures (P), temperatures (T), volumes (V) and compositions (x) of components, offering a theoretically strict way to calculate various thermodynamic properties, such as phase equilibrium and *PVTx* properties, which are important in a wide range of geochemical applications. The parameters of an EOS are generally evaluated from experimental data. With the advent of MD/MC simulations, the *PVT* data of computer simulation, together with experimental data, are also used for improving EOS (Belonoshko and Saxena, 1991; Brodholt and Wood, 1993; Duan et al., 1992b).

The EOS of Brodholt and Wood (1993) was based on the experimental data available then and the simulations of TIP4P model. Since then, new experimental data (Abramson and Brown, 2004; Brodholt and Wood, 1994; Frost and Wood, 1997; Larrieu and Ayers, 1997; Withers et al., 2000) above 2.5 Gpa up to 5.0 Gpa have been published. In order to develop an EOS representing new experimental data and the simulated results of SPCE of this study, we propose the following EOS on the basis of Duan et al. (1992a).

We formulate the EOS based on Duan et al. (1992a):

$$Z = \frac{PV}{RT} = 1 + \frac{B}{V_r} + \frac{C}{V_r^2} + \frac{D}{V_r^4} + \frac{E}{V_r^5} + \left(\frac{F}{V_r^2} + \frac{G}{V_r^4}\right) \exp\left(-\frac{\gamma}{V_r^2}\right) \tag{9}$$

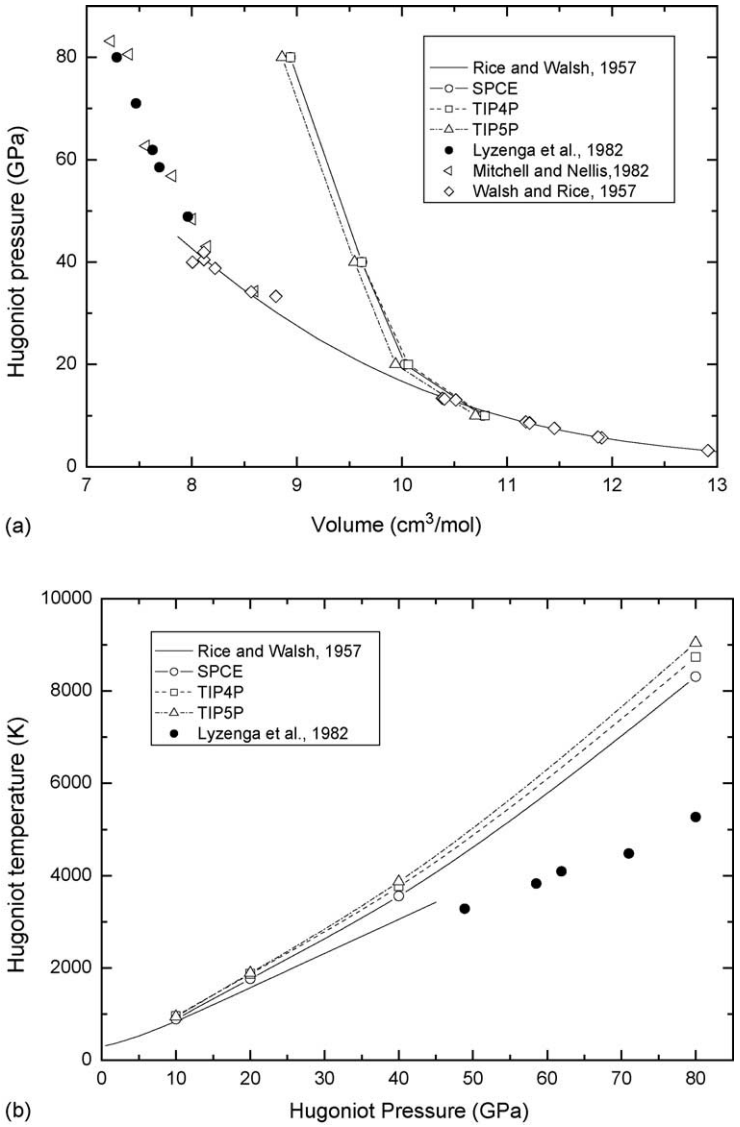

Fig. 5. Simulated data points obeying the Hugoniot relation and a comparison with experimental data determined from the shock wave measurements.

$$B = a_1 + \frac{a_2}{T_r^2} + \frac{a_3}{T_r^3} \tag{10a}$$

$$C = a_4 + \frac{a_5}{T_r^2} + \frac{a_6}{T_r^3} \tag{10b}$$

$$D = a_7 + \frac{a_8}{T_r^2} + \frac{a_9}{T_r^3} \tag{10c}$$

$$E = a_{10} + \frac{a_{11}}{T_r^2} + \frac{a_{12}}{T_r^3} \tag{10d}$$

$$F = \frac{a_{13}}{T_r} \tag{10e}$$

$$G = a_{14} T_r \tag{10f}$$

$$T_r = \frac{T}{T_c} \tag{11}$$

Table 5
Parameters for Eqs. (9) and (10a)–(10f)

a_1	3.49824207D−01
a_2	−2.91046273D+00
a_3	2.00914688D+00
a_4	1.12819964D−01
a_5	7.48997714D−01
a_6	−8.73207040D−01
a_7	1.70609505D−02
a_8	−1.46355822D−02
a_9	5.79768283D−02
a_{10}	−8.41246372D−04
a_{11}	4.95186474D−03
a_{12}	−9.16248538D−03
a_{13}	−1.00358152D−01
a_{14}	−1.82674744D−03
γ	1.05999998D−02

$$V_r = \frac{V}{V_c} \tag{12}$$

where $T_c = 647.25$ K and $V_c = 55.9480373$ cm^3/mol are the critical temperature and volume of water, respectively, $R = 83.14467$ cm^3 bar/(K mol) is the universal gas constant. Parameters for this EOS were tabulated in Table 5. The parameters, a_1–a_{14}, in the above equation, are evaluated from our simulated data (Table 6) and experimental data of liquid above 273.15 K and pressures above 100 MPa. Shock wave data were excluded for their large uncertainties and possible inconsistence with static measured experimental data (Wagner and Prub, 2002). Compared with the simulated data listed in Table 6, the calculated volumes from our EOS show remarkable accuracy with an average relative error of 0.27% and maximum error of 1.75%. At the same time, the calculated volumes are also in good agreement with experimental data from 100.0 MPa up to 5.0 GPa with an average relative error less than 0.5% and maximum error less than 4.0%. Fig. 6 gives the errors of the EOS proposed by Brodholt and Wood (1993) and the EOS in this paper relative to the most recently published *PVT* data (Abramson and Brown, 2004; Brodholt and Wood, 1994; Frost and Wood, 1997; Larrieu and Ayers, 1997; Withers et al., 2000). From this figure, our EOS shows overall better agreement with experiments.

From previous studies, either from experiments (Hamann, 1981) or from ab initio calculations (Cavazzoni et al., 1999), the ionization effect becomes significant to about 20–30 GPa and 2000 K. Accord-

Table 6
Simulated volumes of SPCE to high temperatures and pressures

T (K)	P (MPa)	V (cm^3/mol)	ΔV (cm^3/mol)
523.15	5000	12.08	0.01
773.15	1500	16.37	0.04
773.15	2000	15.38	0.03
773.15	2500	14.72	0.04
773.15	3000	14.14	0.03
773.15	3500	13.71	0.03
773.15	4000	13.33	0.02
773.15	4500	13.02	0.02
773.15	5000	12.73	0.01
773.15	5500	12.5	0.02
773.15	6000	12.27	0.02
773.15	6500	12.07	0.02
773.15	7000	11.88	0.02
873.15	1500	17.03	0.07
873.15	2000	15.91	0.03
873.15	2500	15.11	0.04
873.15	3000	14.51	0.01
873.15	3500	14.04	0.03
873.15	4000	13.63	0.02
873.15	4500	13.29	0.03
873.15	5000	13	0.01
873.15	5500	12.73	0.03
873.15	6000	12.51	0.01
873.15	6500	12.28	0.02
873.15	7000	12.1	0.01
873.15	7500	11.91	0.03
873.15	8000	11.75	0.01
973.15	1000	19.68	0.08
973.15	1500	17.67	0.08
973.15	2000	16.4	0.04
973.15	2500	15.55	0.05
973.15	3000	14.89	0.04
973.15	3500	14.36	0.04
973.15	4000	13.94	0.02
973.15	4500	13.56	0.01
973.15	5000	13.25	0.03
973.15	5500	12.97	0.02
973.15	6000	12.71	0.02
973.15	6500	12.49	0.02
973.15	7000	12.29	0.02
973.15	7500	12.11	0.01
973.15	8000	11.93	0.01
973.15	8500	11.78	0.02
1073.15	2500	15.98	0.04
1073.15	3000	15.28	0.03
1073.15	3500	14.7	0.04
1073.15	4000	14.24	0.03
1073.15	4500	13.83	0.03
1073.15	5000	13.49	0.02
1073.15	5500	13.2	0.03
1073.15	6000	12.93	0.01
1073.15	6500	12.7	0.02
1073.15	7000	12.48	0.02

Table 6 (*Continued*)

T (K)	P (MPa)	V (cm^3/mol)	ΔV (cm^3/mol)
1073.15	7500	12.27	0.01
1073.15	8000	12.11	0.01
1073.15	8500	11.95	0.02
1073.15	9000	11.78	0.02
1073.15	9500	11.65	0.02
1073.15	10000	11.52	0.01
1173.15	1000	21.65	0.14
1173.15	1500	18.97	0.08
1173.15	2500	16.41	0.07
1173.15	4000	14.53	0.04
1173.15	4500	14.12	0.02
1173.15	5000	13.74	0.02
1173.15	5500	13.43	0.02
1173.15	6000	13.15	0.02
1173.15	6500	12.89	0.02
1173.15	7000	12.66	0.02
1173.15	7500	12.47	0.02
1173.15	8000	12.28	0.02
1173.15	8500	12.1	0.01
1173.15	9000	11.95	0.02
1173.15	9500	11.8	0.02
1173.15	10000	11.66	0.01
1173.15	11000	11.41	0.02
1273.15	1500	19.7	0.1
1273.15	2000	17.97	0.03
1273.15	2500	16.89	0.05
1273.15	3500	15.34	0.03
1273.15	4000	14.82	0.04
1273.15	4500	14.37	0.03
1273.15	5000	13.98	0.01
1273.15	5500	13.67	0.02
1273.15	6000	13.36	0.03
1273.15	6500	13.1	0.02
1273.15	7000	12.87	0.03
1273.15	7500	12.64	0.02
1273.15	8000	12.46	0.02
1273.15	8500	12.27	0.02
1273.15	9000	12.11	0.02
1273.15	9500	11.95	0.02
1273.15	10000	11.8	0.01
1273.15	11000	11.54	0.01
1273.15	12000	11.31	0.01
1373.15	1000	23.71	0.16
1373.15	1500	20.43	0.1
1373.15	2000	18.56	0.08
1373.15	4500	14.64	0.04
1373.15	5000	14.23	0.03
1373.15	5500	13.87	0.02
1373.15	6000	13.57	0.02
1373.15	6500	13.29	0.02
1373.15	7000	13.05	0.01
1373.15	7500	12.82	0.02
1373.15	8000	12.62	0.02
1373.15	8500	12.42	0.02

Table 6 (*Continued*)

T (K)	P (MPa)	V (cm^3/mol)	ΔV (cm^3/mol)
1373.15	9000	12.26	0.02
1373.15	9500	12.1	0.01
1373.15	10000	11.95	0.01
1373.15	11000	11.68	0.02
1373.15	12000	11.45	0.01
1373.15	13000	11.21	0.01
1773.15	100	153.69	3.52
1773.15	200	81.57	0.72
1773.15	500	41.08	0.23
1773.15	1000	27.85	0.16
1773.15	2000	20.65	0.05
1773.15	5000	15.18	0.02
1773.15	10000	12.49	0.01
1873.15	1000	28.83	0.15
1873.15	1500	23.85	0.14
1873.15	2000	21.2	0.07
1873.15	3000	18.22	0.07
1873.15	3500	17.29	0.06
1873.15	4000	16.53	0.05
1873.15	4500	15.94	0.03
1873.15	5000	15.42	0.03
1873.15	5500	14.97	0.04
1873.15	6000	14.58	0.05
1873.15	6500	14.24	0.03
1873.15	7000	13.96	0.03
1873.15	7500	13.67	0.02
1873.15	8000	13.43	0.03
1873.15	8500	13.19	0.02
1873.15	9000	12.99	0.03
1873.15	9500	12.79	0.02
1873.15	10000	12.62	0.02
1873.15	11000	12.31	0.01
1873.15	12000	12.02	0.01
1873.15	13000	11.77	0.02
1873.15	14000	11.54	0.01
1873.15	15000	11.34	0.02
1873.15	16000	11.15	0.01
1873.15	17000	10.99	0.01
1873.15	18000	10.82	0.01
1873.15	19000	10.69	0.01
2273.15	100	200.45	4.29
2273.15	200	107.17	2.25
2273.15	500	51.05	0.68
2273.15	1000	32.9	0.27
2273.15	2000	23.28	0.12
2273.15	5000	16.32	0.03
2273.15	10000	13.13	0.02
2273.15	20000	10.85	0.01
2373.15	1000	33.95	0.33
2373.15	1500	27.36	0.16
2373.15	2000	23.72	0.16
2373.15	2500	21.5	0.09
2373.15	3000	20.02	0.14
2373.15	3500	18.84	0.06

Table 6 (*Continued*)

T (K)	P (MPa)	V (cm^3/mol)	ΔV (cm^3/mol)
2373.15	4000	17.91	0.06
2373.15	4500	17.18	0.05
2373.15	5000	16.52	0.05
2373.15	5500	15.98	0.06
2373.15	6000	15.57	0.06
2373.15	6500	15.16	0.04
2373.15	7000	14.77	0.03
2373.15	7500	14.47	0.03
2373.15	8000	14.19	0.03
2373.15	8500	13.9	0.03
2373.15	9000	13.68	0.02
2373.15	9500	13.46	0.03
2373.15	10000	13.26	0.02
2373.15	11000	12.9	0.02
2373.15	12000	12.57	0.02
2373.15	13000	12.29	0.01
2373.15	14000	12.03	0.02
2373.15	15000	11.81	0.01
2373.15	16000	11.6	0.02
2373.15	17000	11.41	0.01
2373.15	18000	11.22	0.01
2373.15	19000	11.07	0.01
2373.15	20000	10.92	0.01
2873.15	1000	38.68	0.44
2873.15	1500	30.46	0.21
2873.15	2000	26.22	0.19
2873.15	2500	23.6	0.21
2873.15	3000	21.69	0.13
2873.15	3500	20.3	0.11
2873.15	4000	19.19	0.08
2873.15	4500	18.35	0.05
2873.15	5000	17.66	0.05
2873.15	5500	17.02	0.07
2873.15	6000	16.46	0.05
2873.15	6500	16	0.04
2873.15	7000	15.62	0.04
2873.15	7500	15.23	0.05
2873.15	8000	14.9	0.05
2873.15	8500	14.62	0.04
2873.15	9000	14.35	0.04
2873.15	9500	14.09	0.04
2873.15	10000	13.87	0.03
2873.15	11000	13.45	0.03
2873.15	12000	13.1	0.02
2873.15	13000	12.78	0.03
2873.15	14000	12.5	0.01
2873.15	15000	12.23	0.01
2873.15	16000	12.02	0.01
2873.15	17000	11.81	0.01
2873.15	18000	11.6	0.03
2873.15	19000	11.43	0.02
2873.15	20000	11.27	0.01
3273.15	200	153.27	2.09
3273.15	500	70.02	0.8
3273.15	1000	42.23	0.32
3273.15	2000	28.08	0.17
3273.15	5000	18.46	0.04
3273.15	10000	14.3	0.02
3273.15	20000	11.52	0.01
3373.15	1000	43.31	0.42
3373.15	1500	33.62	0.2
3373.15	2000	28.68	0.23
3373.15	2500	25.54	0.18
3373.15	3000	23.21	0.12
3373.15	3500	21.74	0.2
3373.15	4000	20.46	0.15
3373.15	4500	19.48	0.04
3373.15	5000	18.71	0.11
3373.15	5500	17.95	0.1
3373.15	6000	17.38	0.06
3373.15	6500	16.8	0.08
3373.15	7000	16.37	0.06
3373.15	7500	15.96	0.04
3373.15	8000	15.61	0.03
3373.15	8500	15.28	0.03
3373.15	9000	14.99	0.03
3373.15	9500	14.69	0.03
3373.15	10000	14.43	0.04
3373.15	11000	13.99	0.04
3373.15	12000	13.57	0.04
3373.15	13000	13.23	0.02
3373.15	14000	12.93	0.02
3373.15	15000	12.65	0.02
3373.15	16000	12.41	0.02
3373.15	17000	12.18	0.02
3373.15	18000	11.96	0.02
3373.15	19000	11.79	0.02
3373.15	20000	11.6	0.01
4273.15	100	372.84	6.59
4273.15	200	194.09	2.79
4273.15	500	86.55	1.37
4273.15	1000	51.14	0.54
4273.15	2000	32.56	0.22
4273.15	5000	20.41	0.06
4273.15	10000	15.39	0.02
4273.15	20000	12.15	0.01
4273.15	50000	9.28	0.01

These *PVT* data were used to propose a new EOS in this study as a supplement to the available experimental data. ΔV is the uncertainty of corresponding volume.

ing to our calculation of Hugoniot curves (Fig. 5), we can get similar implications. So, we believe that this EOS can be used to predict volumes of liquid and compressed water from 273.15 K and 100 MPa to 2000 K and 20 GPa.

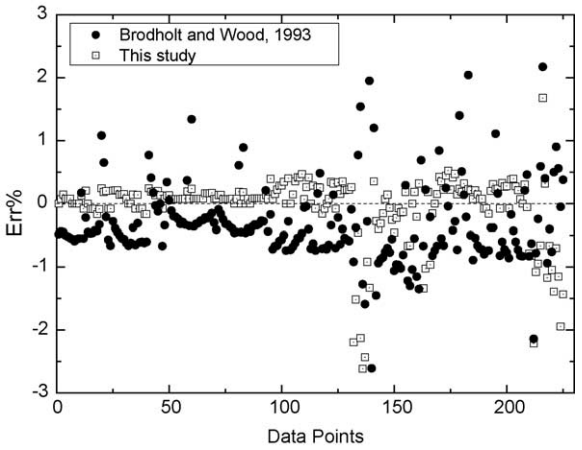

Fig. 6. The relative errors of the EOS proposed by Brodholt and Wood (1993) and the EOS in this paper comparing with all the recent published *PVT* data (Abramson and Brown, 2004; Brodholt and Wood, 1994; Frost and Wood, 1997; Larrieu and Ayers, 1997; Withers et al., 2000).

5. Conclusion

In order to study the *PVT* properties of water at high temperatures and pressures and demonstrate the validity of MD/MC simulation, we systematically performed a series of isothermal–isobaric molecular dynamics simulations to comprehensively evaluate the *PVT* properties of water with four popular pairwise additive models, SPCE, TIP4P, TIP5P and EP. From the overview of the simulated data and their comparisons with experimental data, we find that SPCE shows overall better predictions than the other three models, slightly more accurate than TIP4P (Fig. 6), but far more accurate than EP and TIP5P. Compared with the most recent published high-pressure experimental data, simulation results with SPCE show remarkable agreement with errors less than 1.0% (Fig. 3). Considering that SPCE was developed based on very few experimental data under normal temperatures and pressures, the high accuracy of the simulation results indicate a great predictive power of molecular level study and demonstrated the validity of molecular dynamics simulations to generate data as an important supplement to the database of thermodynamic properties of geological fluids.

Among the four models, TIP5P and EP can be regarded as descendent models of TIP4P and SPCE, respectively. Unfortunately, these two models were proved to be even inferior to their predecessors in predicting the *PVT* properties. Besides some historical reasons of erroneous details of early simulations, the simple adjustments of pairwise additive potentials seem to be hard or even impossible to improve overall simulated properties. EP, with original purpose to reproduce accurate phase behavior of water, turned out to significantly overestimate the volumetric properties of liquid and compressed water. SPCE, on the other hand, was proven to be very successful at least in the region of condensed water. Considering its remarkable accuracy of dielectric constants over wide range of temperatures and pressures (Wasserman et al., 1994) and reasonable phase behaviors (Guissani and Guillot, 1993), it is therefore suitable for our further study of geological fluids.

Based on our simulated data of SPCE and experimental data, a new EOS was proposed with better accuracy for the volumetric properties of liquid than previous models from 273.15 K and 100.0 MPa up to the substantial ionization limit, which is about 20–30 GPa and 2000 K according to previous studies (Cavazzoni et al., 1999; Hamann, 1981; Schwegler et al., 2001).

Acknowledgements

We'd like to thank Dr. Jiawen Hu for his help on the equation of state in this paper. This work is supported by Zhenhao Duan's 'Hundred Scientists Project' funds awarded by the Chinese Academy of Sciences and his Outstanding Young Scientist Funds (#40225008) awarded by National Science Foundation of China.

Appendix A. Velocity Verlet integration of equations of motion

The velocity Verlet integrator for the equations of motion, Eqs. (1a)–(1d), can be written in two steps:

In the first step, positions r_i and barostat variable η are propagated from t to $t+\Delta t$ (abbreviated in the following as τ for convenience), while $\dot{r}_i$, ξ and $\dot{\eta}$ are temporarily renewed from t to $t+\Delta t/2$ (τ_0) in the following sequence:

$$V(t) = \exp[3\eta(t)] \tag{A.1a}$$

$$T_{\text{inst}}(t) = \frac{\sum_i m_i(\dot{r}_i(t) - \dot{\eta}(t)r_i(t))^2}{k_B f} \tag{A.1b}$$

$$\ddot{\eta}(t) = \frac{[P_{\text{inst}}(t) - P_{\text{desire}}] \times V(t)}{t_p^2 k_B T_{\text{desire}}} + \frac{T_{\text{inst}}(t)}{t_p^2 T_{\text{desire}}} - \xi(t)\dot{\eta}(t) \tag{A.1c}$$

$$\ddot{r}_i(t) = \frac{F_i(t)}{m_i} + \dot{\eta}(t)^2 r_i(t) + \ddot{\eta}(t) r_i(t) - \left[\xi(t) + \frac{3\dot{\eta}(t)}{f}\right][\dot{r}_i(t) - \dot{\eta}(t)r_i(t)] \tag{A.1d}$$

$$r_i(\tau) = r_i(t) + \dot{r}_i(t)\Delta t + \frac{\ddot{r}_i(t)\Delta t^2}{2} \tag{A.1e}$$

$$\eta(\tau) = \eta(t) + \dot{\eta}(t)\Delta t + \frac{\ddot{\eta}(t)\Delta t^2}{2} \tag{A.1f}$$

$$\dot{r}_i(\tau_0) = \dot{r}_i(t) + \frac{\ddot{r}_i(t)\Delta t}{2} \tag{A.1g}$$

$$\xi(\tau_0) = \xi(t) + \frac{[f k_B T_{\text{inst}}(t) + 3\dot{\eta}(t)^2 t_p^2 k_B T_{\text{desire}} - (f+1)k_B T_{\text{desire}}]\Delta t}{2Q} \tag{A.1h}$$

$$\dot{\eta}(\tau_0) = \dot{\eta}(t) + \frac{\ddot{\eta}(t)\Delta t}{2} \tag{A.1i}$$

where $T_{\text{inst}}(t)$ is the instantaneous temperature at t time.

Then, volume is renewed with:

$$V(\tau) = \exp[3\eta(\tau)] \tag{A.2}$$

In the second step, $\dot{r}_i$, ξ and $\dot{\eta}$ are propagated from τ_0 to τ:

$$\dot{r}_i(\tau) = \frac{\dot{\eta}(\tau)^2 r_i(\tau)\Delta t}{2} + \dot{\eta}(\tau)r_i(\tau) - \left[\xi(\tau) + \frac{3\dot{\eta}(\tau)}{f}\right] \times \frac{[\dot{r}_i(\tau) - \dot{\eta}(\tau)r_i(\tau)]\Delta t}{2} + \dot{r}_i(\tau_0) - \dot{\eta}(\tau_0)r_i(\tau) + \frac{F_i(\tau)\Delta t}{2m_i} \tag{A.3a}$$

$$\xi(\tau) = \frac{\sum_i m_i[\dot{r}_i(\tau) - \dot{\eta}(\tau)r_i(\tau)]^2\Delta t}{2Q} + \frac{3t_p^2 k_B T_{\text{desire}}\dot{\eta}(\tau)^2\Delta t}{2Q} + \xi(\tau_0) - \frac{(f+1)k_B T_{\text{desire}}\Delta t}{2Q} \tag{A.3b}$$

$$\dot{\eta}(\tau) = \frac{\sum_i m_i[\dot{r}_i(\tau) - \dot{\eta}(\tau)r_i(\tau)]^2(1+3/f)\Delta t}{6t_p^2 k_B T_{\text{desire}}} - \frac{\xi(\tau)\dot{\eta}(\tau)\Delta t}{2} + \dot{\eta}(\tau_0) + \frac{[W(\tau) - P_{\text{desire}} \times V(\tau)]\Delta t}{2t_p^2 k_B T_{\text{desire}}} \tag{A.3c}$$

We notice that the variables to be solved ($\dot{r}_i(\tau)$, $\xi(\tau)$ and $\dot{\eta}(\tau)$) appear in both sides of Eqs. (A.3a)–(A.3c), which suggests that an iterative algorithm should be adopted. A possible solution can be achieved with the Newton–Raphson method (Frankel and Smit, 1996).

When the molecules in the simulation are rigid or partially rigid, the constraints on the particle degrees of freedom can be handled using the RATTLE algorithm (Andersen, 1983). As the time derivative of position rather than the velocity was used in our proposed algorithm, the original description of RATTLE can be directly used without any further modifications. However, attention should be paid that RATTLE should be part of the iterative procedure since the constraint virial would affect the calculated $\dot{\eta}(\tau)$ (Eq. (A.3c)) and the other variables ($\dot{r}_i(\tau)$ and $\xi(\tau)$) as a result.

References

Abramson, E.H., Brown, J.M., 2004. Equation of state of water based on speeds of sound measured in the diamond-anvil cell. Geochim. Cosmochim. Acta 68 (8), 1827–1835.

Allen, M.P., Tildesley, D.J., 1989. Computer Simulation of Liquids. Oxford Science Publications, Oxford.

Andersen, H.C., 1980. Molecular dynamics simulations at constant pressure and/or temperature. J. Chem. Phys. 72 (4), 2384–2393.

Andersen, H.C., 1983. Rattle: a "velocity" version of the Shake algorithm for molecular dynamics calculations. J. Comput. Phys. 52, 24–34.

Belonoshko, A., Saxena, S.K., 1991. A molecular dynamics study of the pressure–volume–temperature properties of super-critical fluids. I. H_2O. Geochim. Cosmochim. Acta 55, 381–387.

Berendsen, H.J.C., Grigera, J.R., Straatsma, T.P., 1987. The missing term in effective pair potentials. J. Phys. Chem. 91, 6269–6271.

Bridgman, P.W., 1942. Freezing parameters and compressions of twenty-one substances. Proc. Am. Acad. Arts Sci. 74, 419.

Brodholt, J., Wood, B., 1993. Simulations of the structure and thermodynamic properties of water at high pressures and temperatures. J. Geophys. Res. 98, 519–536.

Brodholt, J.P., Wood, B.J., 1994. Measurements of the *PVT* properties of water to 25 kbars and 1600 °C from synthetic fluid inclusions in corundum. Geochim. Cosmochim. Acta 58 (9), 2143–2148.

Cavazzoni, C., et al., 1999. Superionic and metallic states of water and ammonia at giant plant conditions. Science 283, 44–46.

Ciccotti, G., Ferrario, M., Ryckaert, J.P., 1982. Molecular dynamics of rigid systems in Cartesian coordinates: a general formulation. Mol. Phys. 47 (6), 1253–1264.

Ciccotti, G., Martyna, G.J., Melchionna, S., Tuckerman, M.E., 2001. Constrained isothermal–isobaric molecular dynamics with full atomic virial. J. Phys. Chem. B 105, 6710–6715.

Duan, Z., Moller, N., Weare, J.H., 1992a. An equation of state (EOS) for CH_4—CO_2—H_2O. I: pure systems from 0 to 1000 °C and from 0 to 8000 bar. Geochim. Cosmochim. Acta 56, 2605–2617.

Duan, Z., Moller, N., Weare, J.H., 1992b. Molecular dynamics simulation of *PVT* properties of geological fluids and a equation of state of non-polar and weakly polar gases up to 2000 K and 20,000 bar. Geochim. Cosmochim. Acta 56, 3839–3845.

Duan, Z., Moller, N., Weare, J.H., 1996. A general equation of state for supercritical fluid mixtures and molecular dynamics simulation of mixture *PVTX* properties. Geochim. Cosmochim. Acta 60 (7), 1209–1216.

Errington, J.R., Panagiotopoulos, A.Z., 1998. A fixed point charge model for water optimized to the vapor–liquid coexistence properties. J. Phys. Chem. B 102, 7470–7475.

Finney, J.L., 2001. The water molecule and its interactions: the interaction between theory, modelling, and experiment. J. Mol. Liq. 90, 303–312.

Franck, M.R., Fei, Y.W., Hu, J.Z., 2004. Constraining the equation of state of fluid H_2O to 80 GPa using the melting curve, bulk modulus, and thermal expansivity of ice VII. Geochim. Cosmochim. Acta 68 (13), 2781–2790.

Frankel, D., Smit, B., 1996. Understanding Molecular Simulation: From Algorithms To Applications. Academic Press.

Frost, D.J., Wood, B.J., 1997. Experimental measurements of the properties of H_2O–CO_2 mixture at high pressures and temperatures. Geochim. Cosmochim. Acta 61, 3301–3309.

Guillot, B., 2002. A reappraisal of what we have learnt during three decades of computer simulations on water. J. Mol. Liq. 101 (1–3), 219–260.

Guillot, B., Guissani, Y., 2001. How to build a better pair potential for water. J. Chem. Phys. 114 (15), 6720–6733.

Guissani, Y., Guillot, B., 1993. A computer simulation study of the liquid–vapor coexistence curve of water. J. Chem. Phys. 98 (10), 8221–8235.

Hamann, S.D., 1981. Properties of electrolyte solutions at high pressures and temperatures. In: Rickard, D.T., Wickman, F.E. (Eds.), Physics and Chemistry of the Earth. Oxford, pp. 89–112.

Head-Gordon, T., Hura, G., 2002. Water structure from scattering experiments and simulation. Chem. Rev. 102, 2651–2670.

Hoover, W.G., 1986. Constant-pressure equations of motion. Phys. Rev. A 34 (3), 2499–2500.

Jorgensen, W.L., Chandrasekhar, J., Madura, J.D., Impey, R.W., Klein, M.L., 1983. Comparison of simple potential functions for simulating liquid water. J. Chem. Phys. 79 (2), 926–935.

Kalinichev, A.G., 2001. Molecular simulations of liquid and supercritical water: thermodynamics, structure, and hydrogen bonding. Rev. Miner. Geochem. 42, 83–130.

Kerrick, D.M., Jacobs, G.K., 1981. A modified Redlich–Kwong equation for H_2O, CO_2, and H_2O–CO_2 mixtures at elevated pressures and temperatures. Am. J. Sci. 281, 735–767.

Kormer, S.B., 1968. Optical study of the characteristics of shock-compressed dielectrics. Sov. Phys. Usp. Eng. Trans. 11, 229–254.

Larrieu, T.L., Ayers, J.C., 1997. Measurements of the pressure–volume–temperature properties of fluids to 20 kbar and 1000 °C: a new approach demonstrated on H_2O. Geochim. Cosmochim. Acta 61 (15), 3121–3134.

Lisal, M., Kolafa, J., Nezbeda, I., 2002. An examination of the five-site potential (TIP5P) for water. J. Chem. Phys. 117 (19), 8892–8897.

Lyzenga, G.A., Ahrens, T.J., Nellis, W.J., Mitchell, A.C., 1982. The temperature of shock-compressed water. J. Chem. Phys. 76, 6282–6286.

Mahoney, M.W., Jorgensen, W.L., 2000. A five-site model for liquid water and the reproduction of the density anomaly by rigid, non-polarizable potential functions. J. Chem. Phys. 112 (20), 8910–8922.

Martyna, G.J., Tobias, D.J., Klein, M.L., 1994. Constant pressure molecular dynamics algorithms. J. Chem. Phys. 101 (5), 4177–4189.

McQueen, R.G., Marsh, S.P., Tayler, J.W., Fritz, J.N., Carter, W.J., 1970. The equation of state of solids from shock wave studies. In: Kinslow, R. (Ed.), High velocity impact phenomena. Academic, New York, p. 293.

Melchionna, S., Ciccotti, G., 1993. Hoover NPT dynamics for systems varying in shape and size. Mol. Phys. 78 (3), 533–544.

Mitchell, A.C., Nellis, W.J., 1982. Equation of state and electrical conductivity of water and ammonia shocked to the 100 GPa (1 Mbar) pressure range. J. Chem. Phys. 76 (12), 6273–6281.

Nose, S., 1984. A molecular dynamics method for simulations in the canonical ensemble. Mol. Phys. 52, 255.

Paschek, D., 2004. Temperature dependence of the hydrophobic hydration and interaction of simple solutes: an examination of five popular water models. J. Chem. Phys. 120, 6674–6690.

Ree, F.H., 1982. Molecular interaction of dense water at high temperature. J. Chem. Phys. 76 (12), 6287–6302.

Rice, M.H., Walsh, J.M., 1957. Equation of state of water to 25 kbars. J. Chem. Phys. 26, 824–830.

Sanz, E., Vega, C., Abascal, J.L.F., MacDowell, L.G., 2004. Phase diagram of water from computer simulation. Phys. Rev. Lett. 92 (25), 255701.

Sato, H., et al., 1991. Sixteen thousand evaluated experimental thermodynamic property data for water and steam. J. Phys. Chem. Ref. Data 20 (5), 1023–1044.

Schwegler, E., Galli, G., Gygi, F., Hood, R.Q., 2001. Dissociation of water under pressure. Phys. Rev. Lett. 87 (26), 265501.

Swope, W.C., Andersen, H.C., Berens, P.H., Wilson, K.R., 1982. A computer simulation method for the calculation of equilibrium constants for the formulation of physical clusters of molecules: application to small water clusters. J. Chem. Phys. 76, 637–649.

Tuckerman, M.E., Liu, Y., Ciccotti, G., Martyna, G.J., 2001. Non-Hamiltonian molecular dynamics: generalizing Hamiltonian phase space principles to non-Hamiltonian systems. J. Chem. Phys. 115 (4), 1678–1702.

Wagner, W., Prub, A., 2002. The IAPWS formulation 1995 for the thermodynamic properties of ordinary water substance for general and scientific use. J. Phys. Chem. Ref. Data 31 (2), 387–535.

Wallqvist, A., Mountain, R.D., 1999. Molecular models of water: derivation and description. Rev. Comput. Chem. 13, 183–247.

Walsh, J.M., Rice, M.H., 1957. Dynamic compression of liquids from measurements of strong shock waves. J. Chem. Phys. 26, 815–823.

Wasserman, E., Wood, B., Brodholt, J., 1994. The static dielectric constant of water at pressures up to 20 kbar and temperatures to 1273 K: experiment, simulations, and empirical equations. Geochim. Cosmochim. Acta 59, 1–6.

Wiryana, S., Slutsky, L.J., Brown, J.M., 1998. The equation of state of water to 200 °C and 3.5 GPa: model potentials and the experimental pressure scale. Earth Planet Sci. Lett. 163, 123–130.

Withers, A.C., Kohn, S.C., Brooker, R.A., Wood, B.J., 2000. A new method for determining the *P–V–T* properties of high-density H_2O using NMR: Results at 1.4–4.0 GPa and 700–1100 °C. Geochim. Cosmochim. Acta 64 (6), 1051–1057.

Zhang, Z., Duan, Z., 2002. Phase equilibria of the system methane–ethane from temperature scaling Gibbs ensemble Monte Carlo simulation. Geochim. Cosmochim. Acta 66 (19), 3431–3439.